Scientific Visualization
Overviews Methodologies Techniques

G. Nielson, H. Müller, and H. Hagen, editors

Chapter 9

Studies in Comparative Visualization of Flow Features

Hans-Georg Pagendarm and Frits H. Post

Abstract. *This chapter introduces two important concepts: feature visualization and comparative visualization. Features are patterns or structures hidden in complex data describing physical phenomena. Comparative visualization is concerned with the analysis of differences and sources of error in a simulation or visualization process. Using examples from fluid dynamics, different types of comparative visualization of flow features are illustrated and analysed. Feature extraction techniques for vortices, shock waves, and skin friction are described, and comparative analysis shows their strengths and weaknesses. Some important lessons may be learned from these examples. Comparative visualization is identified as an important tool for data exploration, which provides incentives for explanations and further investigations, and increases awareness of possible problems within the visualization process itself.*

9.1 Introduction

Comparing results or methods is common practice in scientific research. An absolute measure for the accuracy of a data production or sampling process is not often available from any accepted and practically usable theory. In such cases an estimate of the accuracy or the validity of data may be obtained from a comparison with data of different origin but describing the same physics.

The general idea of comparative visualization [8] is that data from two or more different sources are visualized with the intention to show similarities and differences. Differences in visual appearance can be caused by many factors; we list only a few here:

- different physical phenomena
- different experimental or numerical conditions

- measurement artifacts: noise, sampling resolution, interference with the phenomenon, and so on
- numerical inaccuracies
- different mathematics or logic
- the visualization process

Note that each of these sources of difference can be the goal of a comparative study. We will focus here on comparisons of data from two different sources providing information on the same physical phenomenon, and also on comparison of different visualization techniques providing different views of the same data. Using these scenarios, we will illustrate various techniques and applications of comparison.

Comparison is an established way to raise awareness of users and researchers in visualization towards certain difficulties or sources of error. To illustrate this, we will present three cases of comparative analysis in this chapter. The first two cases are concerned with different visualization techniques for the same data: two techniques for visualization of vortices, and two techniques for detecting shock waves. For these two cases, the same data will be used from a numerical flow simulation for a blunt fin/wedge configuration [2] (see Figure 9.1). The data are a result of a Navier-Stokes solution in a hypersonic flow. In Section 9.2, two techniques for vortex visualization are compared, which produce different results from the same data.

Another significant phenomenon in the same flow field, discussed in Section 9.3, is a pattern of shock waves. The flow is studied to learn more about the interaction of shock waves and complex three-dimensional boundary layers or viscous flows in general. Even though the geometry appears to be simple, an extremely complex three-dimensional flow field is generated.

In a wind tunnel experiment, the vortices of Figure 9.1 can produce characteristic traces on the wall of the fin. These patterns have been visualized in the numerical data as well as in a wind-tunnel experiment. The third case, discussed in Section 9.4, is a direct comparison of these numerical and experimental data, showing the relations between these two types of visualization. The differences found in the initial visual comparison are explained, and a new visualization technique is suggested to verify this.

The purpose of this chapter is to show the role that comparative visualization can play in a critical evaluation of different visualization techniques, and how comparative visualization can help to clarify the relation between experiment and simulation.

9.2 Visualization of Vortices

This first example was chosen to illustrate the influence of the scale of an extracted feature with respect to the scale of the discrete resolution of the data. Two alternative methods to visualize vortices in vector fields are compared and show significantly different results. This makes one of the two methods superior for a given data set. Which method to choose may well vary within a single data set depending on the position within the data. More importantly, this behavior is usually not expected by the user of the visualization method.

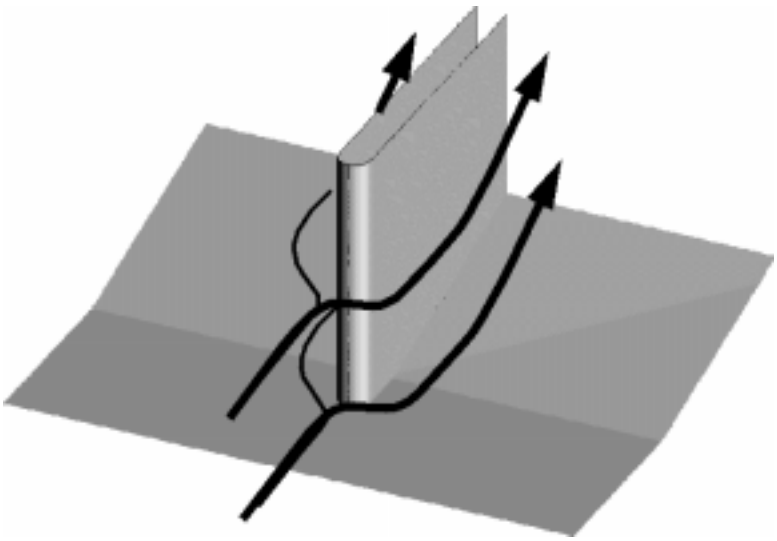

Figure 9.1: Geometry of the flat plate, wedge, and fin configuration placed in a hypersonic flow field (schematic view).

9.2.1 Streamlines and Streamribbons

There is a large number of techniques to analyse and visualize vortical behavior in vector fields (see Banks and Singer [1] for a brief review). In particular in experimental flow visualization, there is a long tradition of visualizing material transport by injection of dye into a water flow [4]. The numerical counterpart of this technique is the calculation of particle paths. Techniques for generating streamlines are well established; for a survey of algorithms, see Kenwright [3]; for implementation issues on streamline integration, see Murman and Powell [5]; for a comparative analysis, see Sadarjoen et al. [10].

However, streamlines can give a poor representation of a complex velocity field, even if they are generated from carefully selected seed points. Figure 9.2 shows a set of streamlines (red and black) which are well placed in order to illustrate the flow characteristics. Exactly the same lines will be used for further analysis in the following images. In spite of the fact that a number of additional yellow and blue lines are used to enhance the image, no deep insight in the flow field is provided. Insertion of even more lines would tend to clutter the image. Streamlines lack a direct representation of swirl, or the streamwise rotational motion of the fluid. This is best represented by vorticity, defined as the curl of velocity, and thus derived from the velocity gradient. Thus, a high density of adjacent streamlines is needed to visualize vorticity.

Consequently, some researchers suggested the use of streamribbons to illustrate this important property of flows. Volpe [13] suggested filling the gap between two streamlines which run more or less in parallel by creating a bundle of lines to give the impression of a solid ribbon. Another way of creating streamribbons is obtained by constructing a mesh of polygons between two adjacent streamlines. We will denote this technique as ‘adjacent

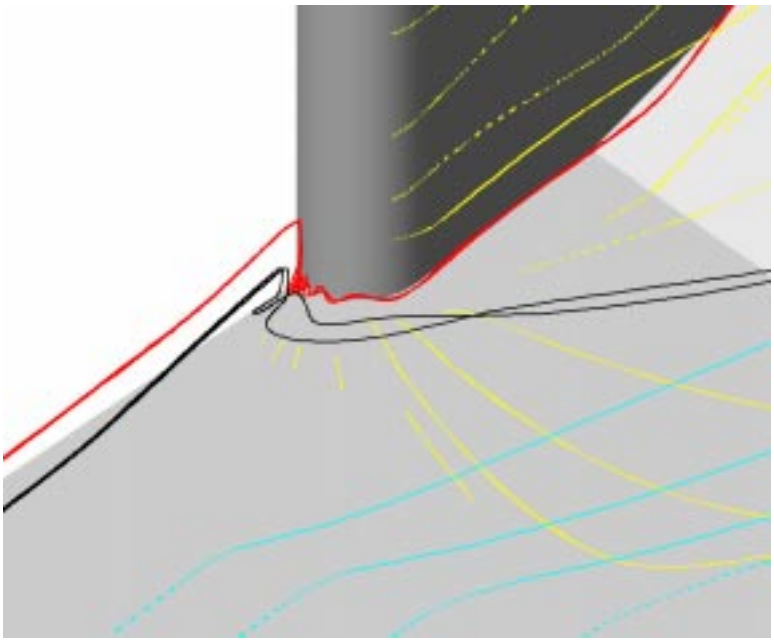

Figure 9.2: Poor representation of a vector field by streamlines.

streamlines' (ASL for short). A simple method to create such a polygon mesh is by the use of a marching triangulation algorithm as described by Pagendarm [6], which demonstrates the problems of such an approach in diverging flow fields.

Divergence of the vector field becomes visible by the increasing width of the ribbons. However, if the two limiting streamlines of the ribbon diverge, they are no longer subject to the same amount of vorticity. They behave quite independently. Since this should not occur for physical reasons, such an event clearly demonstrates the limitations of the method.

These limitations may be overcome by evaluating the data at the location of a single streamline and constructing the ribbon from the angular rotation of the vector field around this line. One way to achieve this is calculating two adjacent streamlines and keeping their distance constant. Such an algorithm may be extracted from Van Wijk [12]. Streamribbons may also be considered as a simplification of a more complex analysis of the stress tensor [11]. For direct comparison to the ASL technique, a straightforward implementation calculating the angular velocity from the curl of the velocity vector field was used [9]. The ribbon is a surface of constant width, centered around a single streamline. The amount of twist of the ribbon is directly linked to angular velocity at the streamline. We will call this the 'twisting ribbon around a single streamline' technique here, or TSR for short.

Figure 9.3 demonstrates, in comparison to Figure 9.2, how the two dominant vortices in the flow field may be intuitively visualized using the TSR method. One would expect that similar information may be extracted from an image constructed using the ASL method (Figure 9.4).

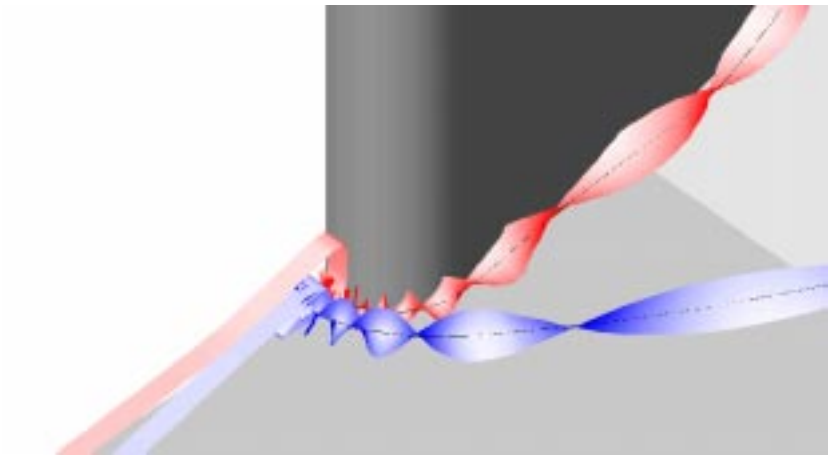

Figure 9.3: Two TSR streamribbons visualize the same data as in Figure 9.2 and clearly depict the axis of two vortices as well as the swirl in the flow. The scale is identical to Figure 9.2.

9.2.2 Evaluation of the Two Techniques

Close examination reveals that the ASL method fails because the two streamlines used for constructing the ribbon do not follow a pure vortical motion, due to interference with other features of the flow. On the other hand, the streamlines converge, which makes it difficult to visualize the vortices without enlargement of the image. Note that the streamlines shown in the image are not incorrect, they just fail to clearly show the desired feature.

The TSR method visualizes pure rotational motion along a single streamline, which is not easily affected by other flow features. It behaves much like an icon depicting the position and swirl of vortices. The scale of the icon (the width of the ribbon) may be adjusted in a wide range to meet the image scale. The ASL method does not allow independent control of the ribbon width, as the width is defined by the paths of the streamlines.

A surface, as defined by two adjacent streamlines connected by a polygon mesh, suggests a linear variation between the streamlines, which may not be warranted at the given distance. The TSR method shows velocity direction and axial rotation, where the latter is a gradient quantity. Approximation of the gradient using finite differences is always linked to local cell size.

In the case of Figure 9.5, a strong enlargement by a factor of 20 is required to make this method useful. The image is expected to show a certain behavior of streamribbons in case vortices are present. Due to the fact that the feature “vortex” is hidden in discrete data, this behavior of ribbons may not occur if an unsuitable method is chosen. In the worst case, the feature is not detectable at all with one of the alternative methods. Note that the method of choice may well be different depending on the data or simply depending on the position within the same data.

In this example, the failure of the ASL method was caused by the need to use stream-

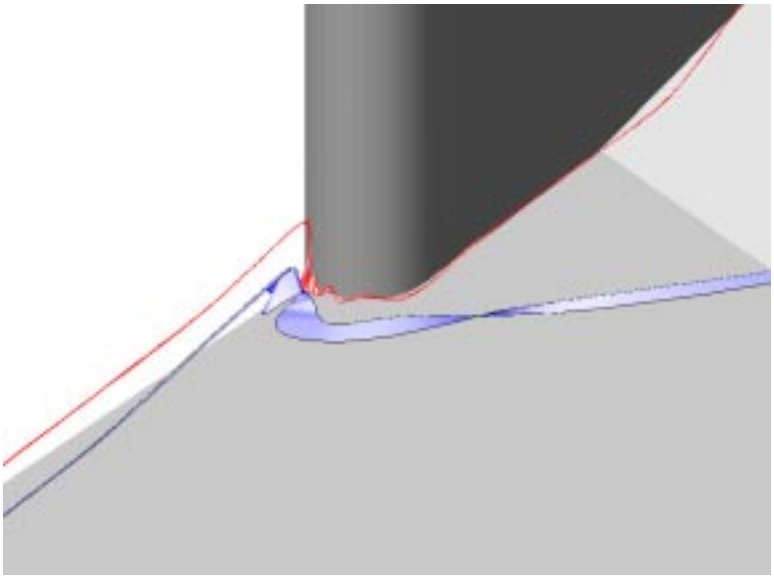

Figure 9.4: The situation of Figure 9.3 visualized by constructing a ribbon from adjacent streamlines, or an ASL ribbon.

lines outside the close proximity of the vortex core in order to meet the requirements of the image scale and make features visible from a distant view. When visualized at the same scale level as the feature, both methods work equally well, however, the TSR method would need further effort to provide additional information such as convergence or divergence in the vector field. The ASL method provides such information implicitly, even down to the size of numerical grid cells.

Going down to very small scales in the range of one or two grid cells, one may find that ribbons constructed from two adjacent streamlines may still pick up small but significant differences in the velocity field. Figure 9.6 illustrates this effect by connecting a number of such ribbons combined to a stream surface which eventually forms an “S”-shape. However, the TSR method does not respond to variation in the vector field at this scale because the evaluation of the curl uses the data values at the vertices of eight adjacent cells, which has a smoothing effect.

For the example of visualizing vortical behavior by streamribbons, one could conclude that the TSR method is superior for small-scale features in large images. When the size of the image is of the same order as the size of the vortex, both methods compared perform well. However, the ASL method can provide additional information about divergence or convergence of the vector field. At scales on the order of grid cells, the TSR method would be preferred to detect physical features, while the ASL method would provide information about the numerical smoothness of the data. The important message is that there is no general rule to select one of the two methods in question and that conditions may well vary within a single data set.

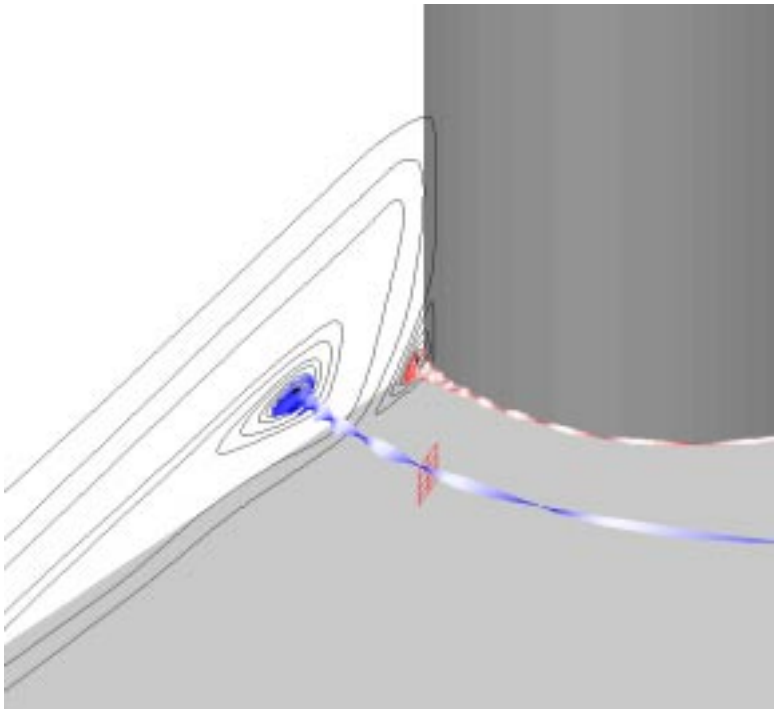

Figure 9.5: ASL streamribbons provide useful visualization if they are used within the proximity of the vortex core where the flow is clearly dominated by vortical effects. Some cells of the numerical grid are shown in the image to emphasize that the relevant region is restricted to a very small scale of a few cells in these data.

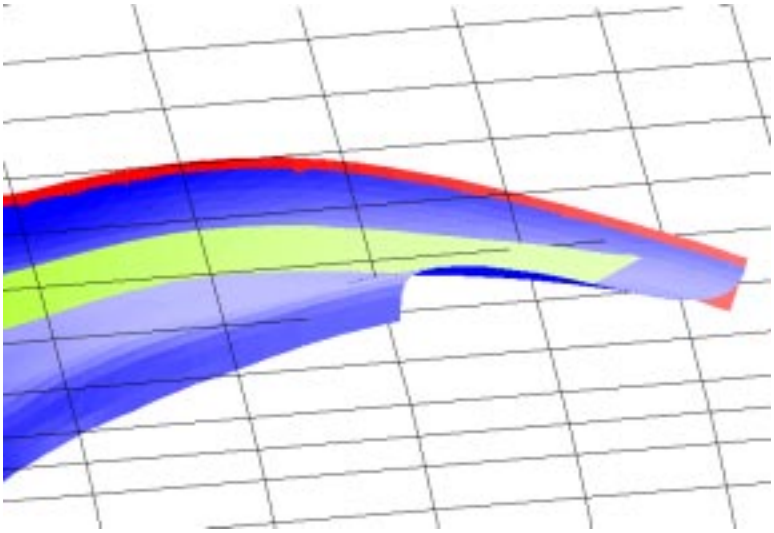

Figure 9.6: The blue stream surface is constructed from 30 adjacent streamlines. While the red ribbon picks up the vortical motion of the flow correctly, the green ribbon fails because of the limited numerical resolution.

In cases where a large number of distributed vortices need to be visualized, there would be a need for more complex visualization techniques. For example, Banks and Singer [1] suggested a method for vortex extraction from complex flow fields such as turbulent shear layers.

9.2.3 Techniques of Comparative Visualization

Comparative visualization may be used to uncover hidden discrepancies between different data intended to describe the same physical phenomena [8]. This approach assumes that the visualization methods used do not introduce significant errors or discrepancies which might affect the resulting comparative analysis. However, it is important to note that various visualization methods which can, in principle, visualize the same phenomenon in the data may well give different results. This effect may also be studied using comparative visualization techniques (see Figure 9.7).

The comparison may be done by presenting images side-by-side, such as Figures 9.3 and 9.4. If the visualization system allows combination of the resulting representations at the level of 3D graphical objects, the object created by the visualization pipeline may be placed within the same image, as was done in Figure 9.6.

The example in the next section will illustrate how two different methods to extract and visualize a three-dimensional shock wave produce a significantly different result. Again, the resulting shock waves may be compared by putting images side-by-side, which already reveals major differences between the two methods used. However, integrating both resulting graphical objects into a single visualization illustrates the significance of the dif-

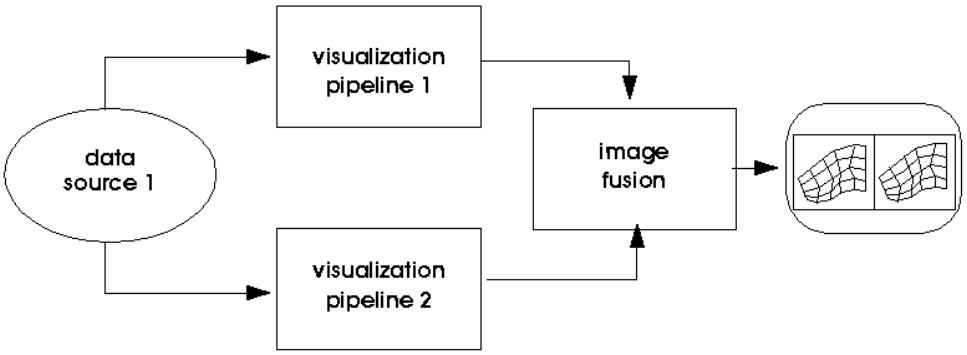

Figure 9.7: Comparing visualization methods.

ferences. Further discussions explain the reason for those differences, as well as their significance for investigation of the underlying physics.

9.3 Visualization of Shock Waves

Returning to the same flow field as used for the vortex visualization, a second dominant feature, a pattern of shock waves in the same data will be visualized.

Since one of the vortex visualization techniques (Section 9.2), is capable of visualizing the vortex seen from greater distances, one might eventually combine the vortex visualization with the visualization of a large-scale shock wave. We will concentrate on the less complex shock visualization here.

The flow in the example approaches from the left with a supersonic speed equivalent to a Mach-number of five. It then hits the wedge at the bottom as well as the blunt fin. Both obstacles cause a complex pattern of shock waves in the flow field. Physically, a shock is marked by an abrupt change in Mach-number. Ahead of the shock, the Mach-number is essentially undisturbed and equal to the free-stream value of five. This is valid for the first or front shock wave in the field. A useful method to find the position of the shock wave in the data is to calculate an isosurface for a Mach-number slightly below the free-stream value (Figure 9.8).

Obviously, in a discrete representation of the flow field, a shock wave is never sharply defined. The method, therefore, visualizes the onset of a transition to a lower Mach-number, which may be spread over several grid cells in streamwise direction. This method can only find the first shock wave at the front, where the deviation from the constant free-stream value occurs, and the Mach-number at the shock is known. The surface is then visualized as a Mach-isosurface. At secondary shocks, the Mach-number is unknown, and isosurface extraction is not possible.

A second shock visualization method [7] locates the local maxima of the gradient of the Mach-number and constructs a surface at these positions. This method is not restricted to locating the first shock wave, but it is able to find any shock in the field. Note that if shocks were represented by sharp discontinuities, both methods would show the same surface.

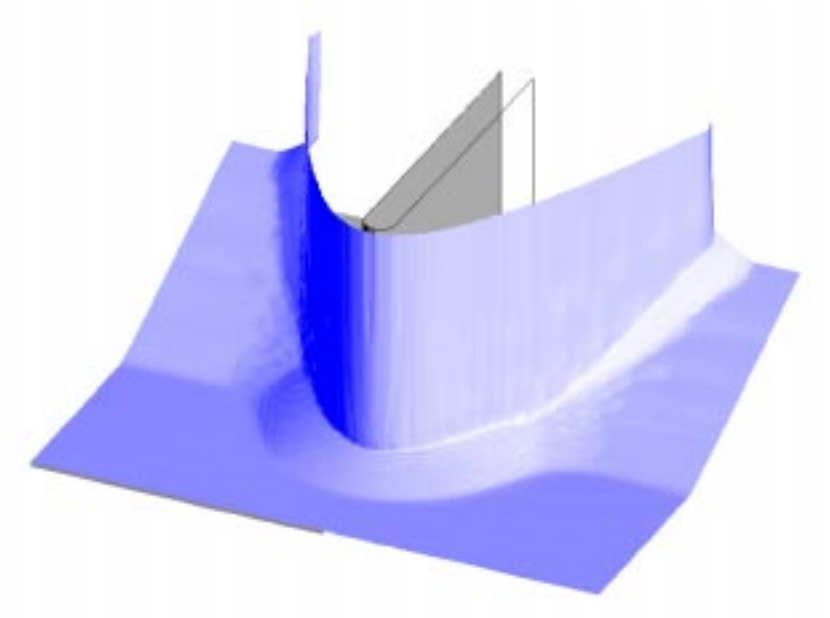

Figure 9.8: Front shock wave visualized using an isosurface close to the free-stream Mach-number. The flow field is the same as in Figures 9.2–9.6.

Again, both alternative methods considered separately (Figures 9.8 and 9.9) provide an acceptable visualization of the shock feature. Once both surfaces are plotted in a single image, a significant spatial displacement becomes visible (Figure 9.10).

There is no physical or mathematical reason to consider either of the two methods incorrect. It is only the discrete representation of the phenomenon in the data that leads to the spatial displacement depending on the algorithm used. Users of visualization software typically are unaware of this type of mismatch between the continuous physical reality and the discrete representation of features in their data. This occurs because the effects are unexpectedly larger than the numerical inaccuracy or noise in the data which is quantified by order-of-accuracy evaluations or noise estimates.

In many cases, comparison of data may only be possible at the image level, that is, by putting images side-by-side (Figure 9.11a). However, as the previous example clearly showed, more detailed information may be obtained when two representations are fed into a common visualization pipeline (Figure 9.11b). In this way we can ensure that the differences we see are not caused by errors in the visualization process. A framework of comparative visualization was given by Pagendarm and Post [8].

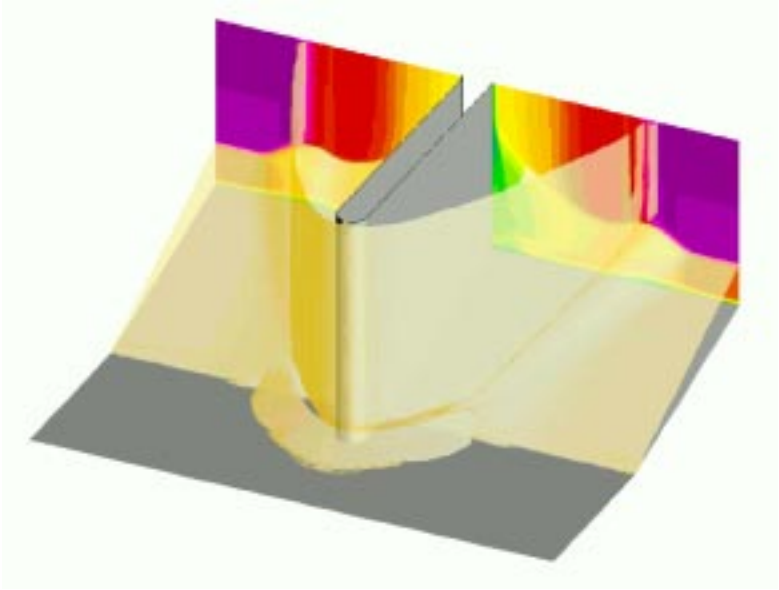

Figure 9.9: Shock wave computed from the location of the maximum local gradient. This method allows us to visualize a secondary shock wave which is visible behind the transparent front shock.

9.4 Visualization of Near-Wall Flow Fields: Simulation and Experiment

In this section we will show examples of comparative visualization in fluid dynamics research using data from different sources. Such sources could be two numerical simulations of the same physics using different algorithms. Obviously, this can be treated similarly to the comparison of visualization algorithms shown above, since data-level comparison is relatively easy to achieve in many cases when the data originates from numerical simulations. Comparative visualization of data from experiments with numerical simulation usually requires a larger effort.

Pagendarm and Walter [9] demonstrated the comparison of near-wall flow fields using oil-flow visualization techniques in a wind tunnel and wall friction lines resulting from a numerical simulation. The use of oil-flow visualization allows global acquisition of near-wall-velocity directional information. The technique employs a dye dispersed in a special oil. This oil is sprayed on the solid walls of the model in the wind tunnel. Due to the viscous action of the flow close to the wall, the oil moves slowly in the local flow direction. When the oil evaporates, it leaves behind a trace of dye, which marks the local flow direction.

In order to compare such experiments with numerical flow simulations, we must visualize a near-wall flow field in a way that is visually comparable to images of the experiment. The direction of a flow velocity field is often visualized using streamlines. In simulations of viscous flows, the velocity of the flow at a solid wall is zero by definition. This prevents the

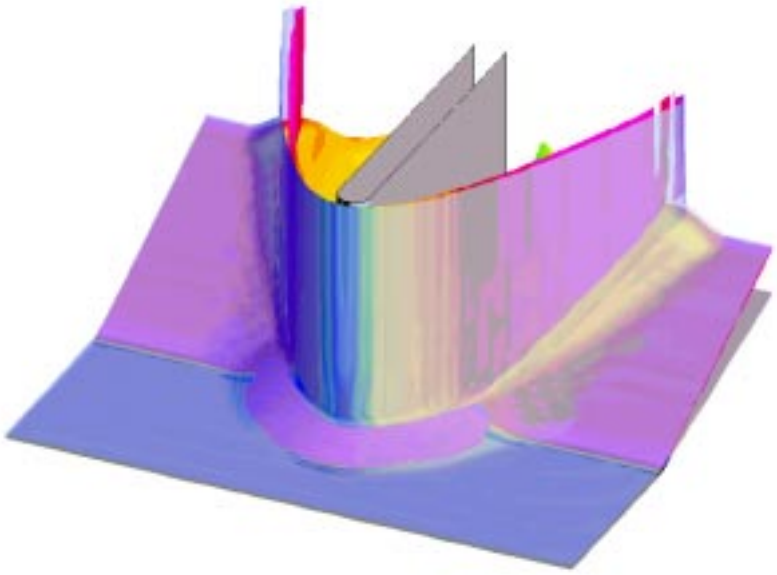

Figure 9.10: Direct comparison of the shock visualization resulting from two alternative methods shows significant spatial displacement of the extracted feature. The blue transparent surface is equivalent to the one in Figure 9.8, the surface behind it matches the golden transparent surface shown in Figure 9.8, and is pseudocolored with Mach-number.

calculation of streamlines directly on the walls. We would like to find the limiting streamline at locations where the velocity goes to zero, while the direction of the velocity vector is determined by the direction of the velocity near the wall. Experienced aerodynamicists will be able to imagine, even qualitatively, the overall three-dimensional flow pattern in the flow field from these wall patterns.

In particular, skin-friction lines show the location of separation and reattachment of the flow at the wall. As mentioned, earlier experiments were performed in a wind tunnel to provide measurements and visualization to match the numerical flow simulation. Oil-flow patterns were recorded photographically. Due to the limited accessibility of the wind tunnel during the experiments, the photograph shows a perspective view of the fin taken from a side of the wind tunnel.

Unfortunately, some of the details of the positions and the equipment used when recording the experiments were no longer available. Therefore, for direct comparison of significant lines and oil-flow pattern, the perspective had to be reconstructed from the edges of the model visible in the image.

After careful matching of the viewing conditions, the skin-friction lines could be projected into the image showing the oil-flow pattern in the wind tunnel experiment. The resulting combined image (Figure 9.13) increases confidence in the overall correctness of the numerical simulation.

Some local discrepancies could be explained by a low grid resolution in the numerical

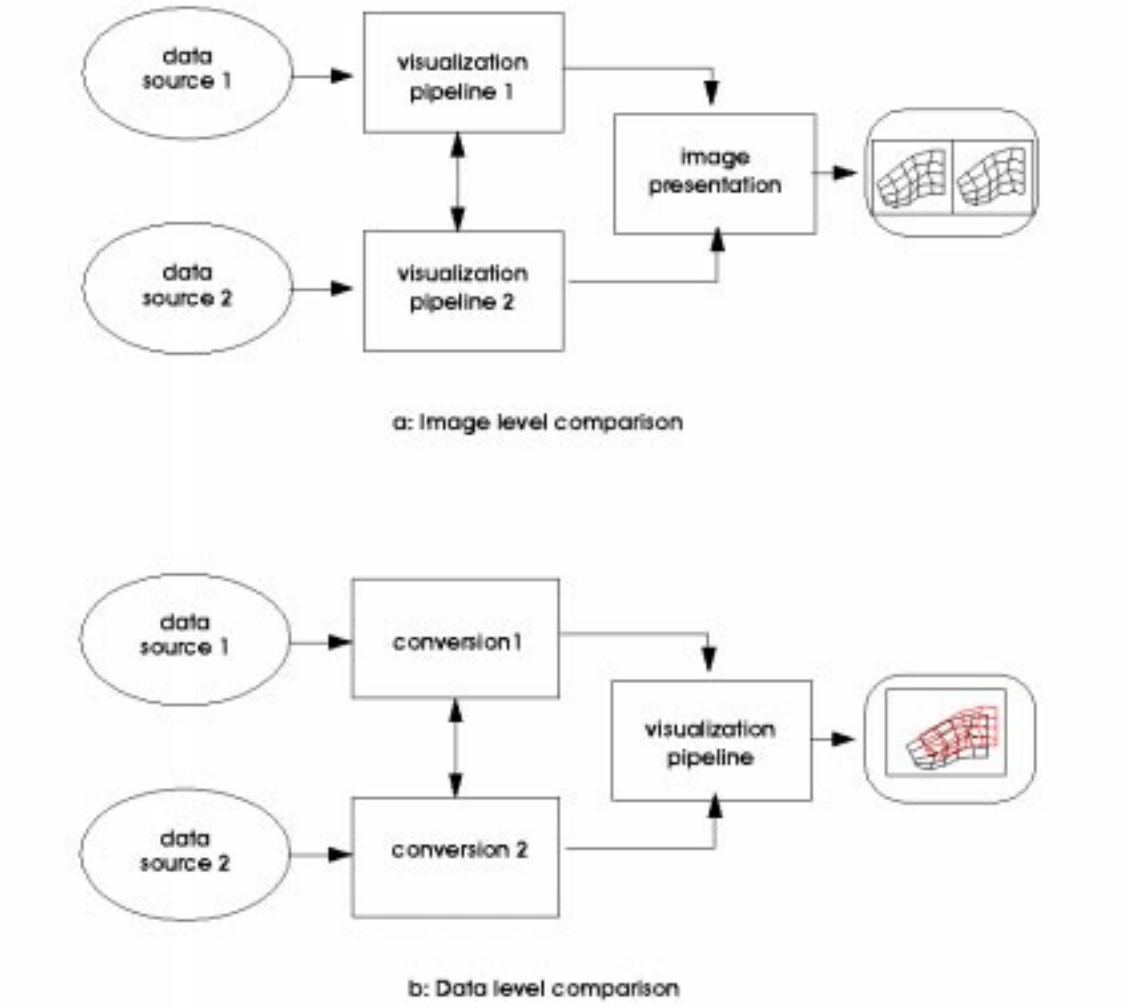

Figure 9.11: Two approaches to comparative visualization [8].

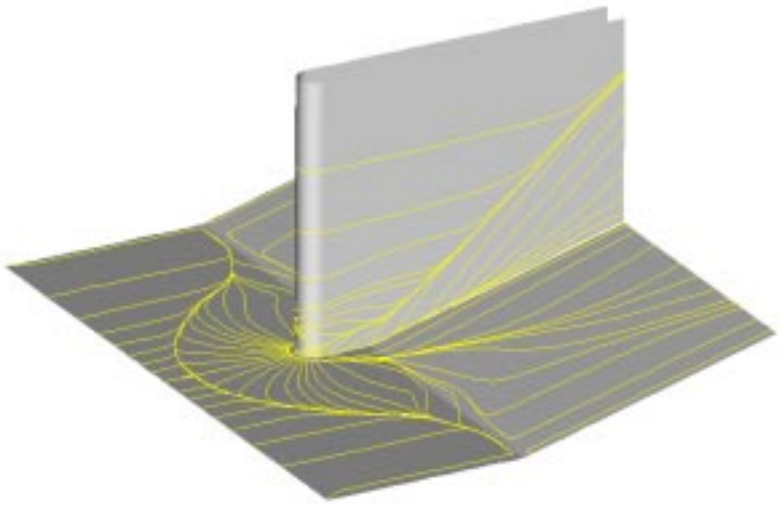

Figure 9.12: Skin-friction lines on walls of the blunt fin and wedge.

simulation. However, the experiment clearly shows a second weak separation line in the lower-side wall of the fin, which does not show up in the numerically generated skin-friction lines (Figure 9.14). The experiment suggests that there is a vortex at some distance from the wall (see Figure 9.3), which is the reason for this pattern.

The flow shows a horseshoe type of vortex. The simulation also reveals a smaller secondary vortex that rotates in the opposite direction. In particular, in the vicinity of the stagnation region ahead of the fin, the vortices are accelerated when they pass the fin. This is advantageous for the visualization since a streamline released in this region is sucked into the vortex and remains very close to the central core for a long time.

Therefore, streamlines were carefully selected to hit the vortex close to the plane of symmetry, then follow the center of the vortex past the fin. The TSR ribbons were calculated for two streamlines, one for each of the vortices.

To find streamlines that stay within the vortex core, the starting point for the streamline must be placed accurately at the center of the vortex. This may be done interactively, or using vortex core detection algorithms (see Banks and Singer [1], and further references in their paper).

The full path of the line consists of two parts: one part integrated forward through the converging vortex core, and a second part that approaches the fin from the inflow boundary, which was integrated backwards to meet the vortex exactly. Careful selection of streamlines and calculation of ribbons allows representation of the vortex pattern with effective and easily perceived visual objects that do not clutter the image (Figure 9.15).

In the case discussed here, the horseshoe vortex passes the fin with increasing distance, while the secondary vortex stays very close to the side wall of the fin. When visualized in combination with the oil-flow pattern obtained in the wind tunnel experiment, the position of this secondary vortex nicely explains the weak trace of a separating flow halfway up the

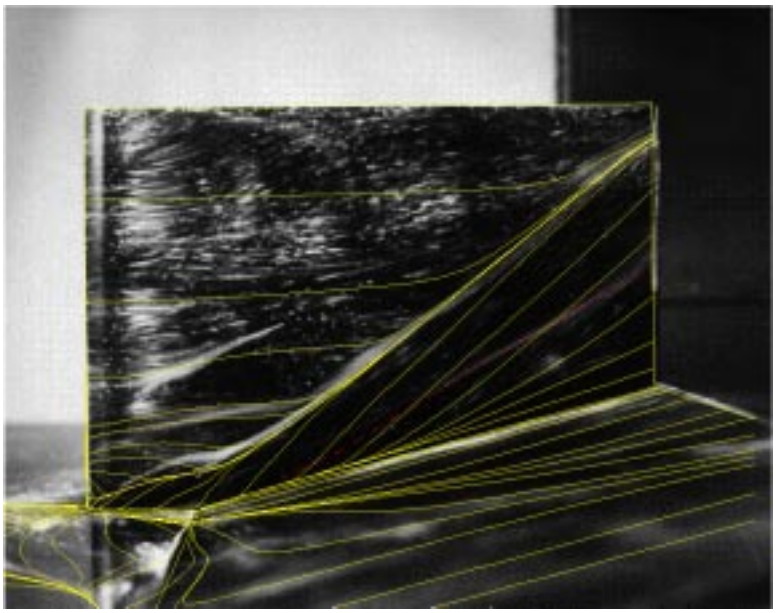

Figure 9.13: Skin-friction lines on walls of the blunt fin and wedge.

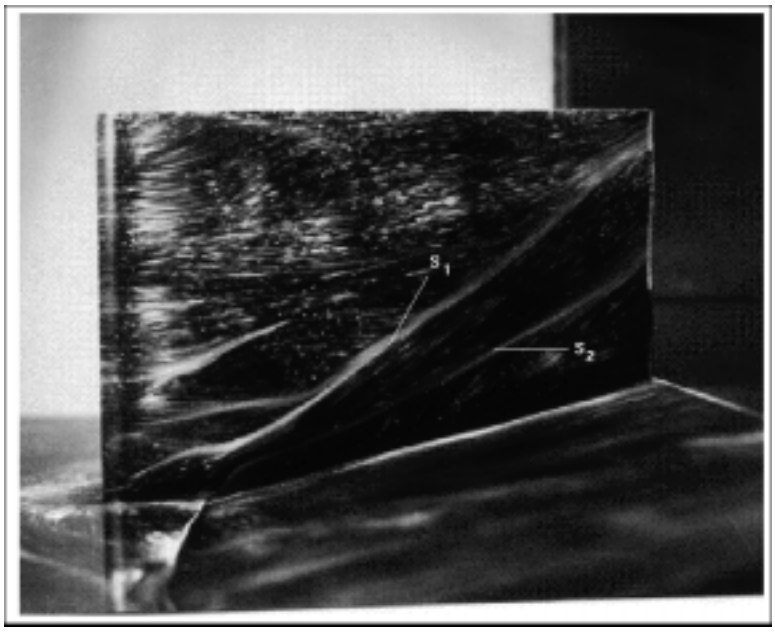

Figure 9.14: The oil-flow pattern shows a second weak separation trace s_2, which is not visible in the numerical data.

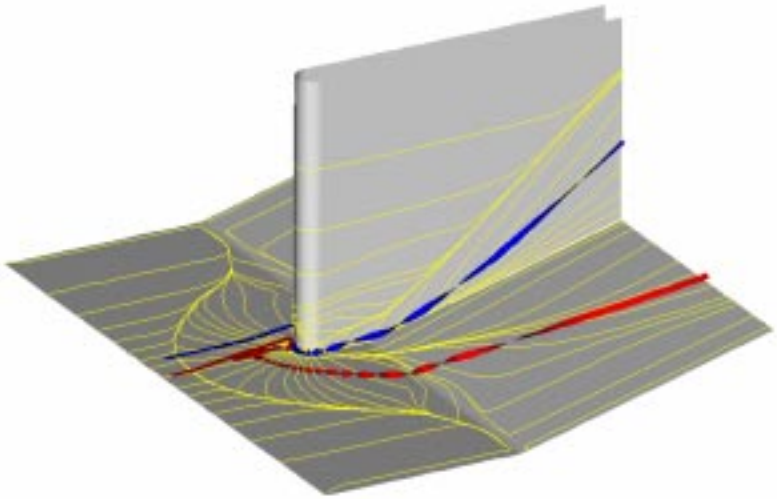

Figure 9.15: Ribbons represent vortices in the flow field. The image allows the examination of three-dimensional phenomena with respect to their traces on the solid walls.

fin. Figure 9.16 shows the vortex core close to the fin, slightly below the lower separation trace. The vortex must be below this trace to explain the topology of the pattern on the fin. As expected, this vortex is only weakly represented, due to low grid resolution in the simulation. This may explain why the skin friction lines as they are shown in Figures 9.12 and 9.13 do not show this separation.

9.5 Discussion and Conclusions

In the three cases described above, a variety of issues in scientific visualization were discussed. First, the problem of evaluating different visualization techniques was discussed. It turns out that this is not just a matter of accuracy; other issues are involved, such as the choice of parameters to be visualized, and the relation between grid resolution and the physical size of features. All of the visualization techniques involved—streamribbons, shock wave surfaces, and skin friction lines—are physically correct and accurate representations, but each technique has its own functionality, and its own conditions of applicability.

A set of adjacent streamlines is a good representation of flow direction, but it does not directly show certain derived quantities, such as rotation or divergence. Using the velocity gradient tensor to derive good approximations of these quantities gives a clear result, and is always linked to grid resolution. However, the gradient quantities are less intuitive and must be visualized separately, whereas the streamlines are a more intuitive and integrated representation. Eventually, a combination of both techniques may be desirable.

The scale of physical features in relation with the size of the visual representation is another interesting issue. Commonly, a trilinear field is assumed within each grid cell, so very complex curves cannot be expected inside a single cell. But, in order to make good

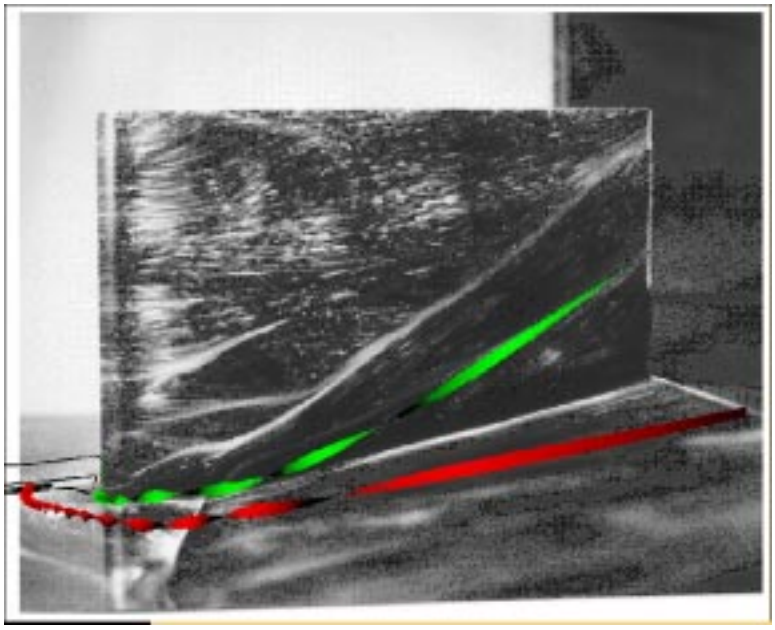

Figure 9.16: Three-dimensional vortex cores from the numerical simulation visualized in combination with oil-flow traces from wind tunnel experiments.

use of computed data, at least one sample should be taken in each cell. So a visualization technique should somehow be linked to the local grid resolution, which is not the case with the adjacent streamlines technique. In the case of the shock waves, the limited resolution of the data smoothes down the important discontinuities, and this introduces a significant difference in detected position, depending on the technique employed. The use of the approximated second derivatives is more general, as it detects all shock waves, but the smoothing effect of the gradient calculation places the shock surface at the center of the transition zone.

The role of comparative visualization is mainly limited to presentation techniques, but the shock wave example in particular shows the value of simultaneous presentation in a single image. Similar techniques such as image fusion and differential display could also be applied for this purpose.

One important lesson is that users should be made more aware of the problems in choosing visualization techniques in a particular case. This is not merely a matter of good or bad, but also of the right conditions of applicability. The example of the near-surface flow suggests that comparing experiment and simulation does not directly lead to a validation of the simulation model. The comparison is mainly performed at the level of features, and the numerical data can be further explored to look for hidden features that do not show up at the first try. This shows that comparative visualization is not a one-time event, but that it initiates an iterative process of matching images, explaining differences, and testing possible explanations using other visualizations. Perhaps the incentive to explain, to generate and test hypotheses is the most important effect of comparison, which lies at the heart of the process of scientific research. Reliable visualization tools and techniques for comparative visualization can help users to concentrate on the underlying physics and simulation models, rather than on the internal problems of the visualization process.

Acknowledgments

This research is a result of the informal cooperation between the authors at DLR in Göttingen and at TU Delft on comparative visualization in CFD research. The data of the blunt fin/wedge configuration were kindly supplied by T. Gerhold [2]. Birgit Walter contributed wall-shear and vortex visualization.

Bibliography

[1] D.C. Banks, B.A.Singer (1994) Vortex Tubes in Turbulent Flows: Identification, Representation, Reconstruction, in: R.D. Bergeron, A.E. Kaufman (eds.) *Proceedings Visualization '94*, IEEE Computer Science Press, pp. 132-139

[2] T. Gerhold (1994) *Numerische Simulation und Analyse der turbulenten Hyperschallströmung um einen stumpfen Fin mit Rampe*, Technical Report DLR-FB 94-19, DLR

[3] D.N. Kenwright (1993) *Dual Stream Function Methods for Generating Three-Dimensional Stream Lines*, PhD Thesis, Department of Mechanical Engineering, University of Auckland, August

[4] W. Merzkirch (1987) *Flow Visualization*, 2nd edition, Academic Press, New York

[5] E. Murman, K. Powell (1989), Trajectory Integration in Vortical Flow, *AIAA Journal*, Vol 27, No. 7, July, pp. 982-984

[6] H.-G. Pagendarm (1991), Flow Visualization Techniques in Computer Graphics, in: *Computer Graphics and Flow Visualization in Computational Fluid Dynamics*, VKI Lecture Series Monograph 1991-07, Von Karman Institute for Fluid Dynamics, Rhode-St.-Genese, Belgium

[7] H.-G. Pagendarm, B. Seitz (1993), An algorithm for Detection and Visualization of Discontinuities in Scientific Data Fields Applied to Flow Data with Shock Waves, in: P. Palamidese (ed.): *Scientific Visualization - Advanced Software Techniques*, Ellis Horwood Ltd., Chichester, UK, pp. 161-177

[8] H.-G. Pagendarm, F.H. Post (1995), Comparative Visualization - Approaches and Examples, in: M. Göbel, H. Müller, B. Urban (eds.) *Visualization in Scientific Computing*, Springer, Wien, pp. 95-108

[9] H.-G. Pagendarm, B. Walter (1994), Feature Detection from Vector Quantities in a Numerically Simulated Hypersonic Flow Field in Combination with Experimental Flow Visualization, in: R.D. Bergeron, A.E. Kaufman (eds.) *Proceedings Visualization '94*, IEEE Computer Science Press, pp. 117-123

[10] A. Sadarjoen, T. van Walsum, A.J.S Hin, F.H. Post (1994), Particle Tracing Algorithms for 3D Curvilinear Grids, in: G. Nielson, H. Müller and H. Hagen (eds.) *Scientific Visualization: Overviews, Methodologies, and Techniques*, IEEE Computer Science Press (this volume)

[11] W.J. Schroeder, C.R. Volpe, W.E. Lorensen (1991), The Stream Polygon: A Technique for 3D Vector Visualization, in: G.M. Nielson, L. Rosenblum (eds.) *Proceedings Visualization '91*, IEEE Computer Society Press, pp. 126-132

[12] J.J. van Wijk (1993), Flow Visualization with Surface Particles, *IEEE Computer Graphics and Applications*, Vol. 13, No. 4, pp. 18-24

[13] G. Volpe (1989), *Streamlines and Streamribbons in Aerodynamics*, AIAA Paper 89-0140, 27th Aerospace Science Meeting, Jan 9-12, Reno, Nevada